Self-Diffusion of Rodlike Polymers in Isotropic Solutions

Zimei Bu, Paul S. Russo,* Debbie L. Tipton, and Ioan I. Negulescu

Department of Chemistry and Macromolecular Studies Group, Louisiana State University, Baton Rouge, Louisiana 70803-1804

Received May 16, 1994; Revised Manuscript Received August 12, 1994®

ABSTRACT: The self-diffusion coefficient, D_s, of fluorescently tagged poly(γ-benzyl α,L-glutamate) has been measured throughout the isotropic regime in pyridine. Intrinsic viscosity, phase boundary studies, epifluorescence microscopy, computer modeling, and the diffusion rates themselves show that the labeling does not appreciably perturb the semiflexible rod structure of the polymer. It is also demonstrated that pyridine is a good solvent for poly(γ-benzyl α,L-glutamate), comparable to *N,N'*-dimethylformamide. As concentration increases, two or three regimes are found depending on the rod length. Dilute behavior holds to number densities, ν, well exceeding L^{-3}, where L is the rod length. A somewhat better estimate of the point at which D_s begins to decrease is the classical criterion, $c \approx [\eta]^{-1}$ where c is the weight/volume concentration and $[\eta]$ is the intrinsic viscosity. Over the whole range of molecular weights, the condition $\nu dL^2 \approx 0.5$–1, where d is the rod diameter, well describes the downturn number density. This corresponds to $\nu/\nu^* \approx 0.1$–0.2, where $\nu^* = 16/(\pi dL^2)$ is the Onsager critical number density associated with the lyotropic liquid crystal transition. Once diffusion begins to decrease, it does so strongly, obeying $D_s \sim c^{-1.13\pm0.04}L^{-1.8\pm0.2}$. The third regime of diffusion, evident only in the two longest samples, is again relatively level and lasts to the lyotropic transition. Diffusion does not cease at any concentration, and D_s is reasonably well scaled when number density is normalized by ν^*, which underscores the importance of finite thickness effects for semidilute solutions of poly(γ-benzyl α,L-glutamate). The self-friction and mutual friction coefficients differ, with the former being lower in dilute solutions.

Introduction

Transport of polymers in melts and concentrated binary solutions has been a major theme in polymer science since its inception. Most studies have concerned random flight polymers, and several reviews are available.[1–3] The mobility of particles with other shapes in various complex environments has also attracted much attention.[4–6] Perhaps the simplest example is the thin, rigid rod.[7,8] Theories for the translational diffusion of rigid rods in nondilute solutions[9–14] begin with the work of Doi and Edwards.[15,16] Several dynamic light scattering (DLS) studies have appeared, but the limitations of this method in nondilute solutions are legendary. Problems such as "slow modes", preparation of ultraclean samples, and, most importantly, the fundamental inability of DLS to measure a self-diffusion coefficient in nondilute solutions led to the popularity of powerful optical diffusion methods such as forced Rayleigh scattering[17] and fluorescence photobleaching recovery (FPR).[18] Nonoptical methods have thrived, too.[6,19]

Despite the commercial, biological, and pedagogical importance of rods, very few self-diffusion studies of stiff polymers have appeared.[20,21] There is no comprehensive study of nonionic polymers in the very stiff limit where the contour length is comparable to or less than the persistence length. The present paper fills this gap. Self-diffusion results determined by the FPR method will be reported for five paucidisperse samples of rodlike poly(γ-benzyl α,L-glutamate) (PBLG) in pyridine solutions spanning the entire isotropic regime.

Theoretical Background

In dilute solution (indicated by a superscript zero) a thin rod diffuses two times more rapidly parallel to its own axis than it does perpendicular to it:[7,22]

$$D_\parallel^0 = 2D_\perp^0 = \frac{3}{2}D^0 \tag{1}$$

where the last relation follows from the expression for the average diffusion coefficient, D^0:

$$D^0 = \frac{1}{3}(D_\parallel^0 + 2D_\perp^0) \tag{2}$$

Doi and Edwards (DE) reasoned that eq 1 would hold at number densities ν less than one rod per volume L^3, where L is the rod length.[15,16] They defined the dilute regime by the inequality $\nu L^3 < 1$. Calculations for typical rods show this to be a remarkably low criterion that would eliminate most polymer characterization methods from consideration. The first clue that it is unrealistic and that entanglement effects in rods in fact are harder to produce than they may seem to be at first, comes from the long history of successful analytical characterizations of rigid-rod polymers.[23,24] Nevertheless, entanglements[25] will occur eventually, to be relaxed when the rods become aligned at some critical concentration ν^* which Onsager predicted to be

$$\nu^* = 16/\pi dL^2 \approx 5/dL^2 \tag{3}$$

where d is the rod diameter. The isotropic, "semidilute" regime was therefore envisioned by DE to span the range $L^{-3} < \nu < d^{-1}L^{-2}$. In this regime, DE assume that $D_\perp$ is reduced to zero by collisions with other rods while $D_\parallel$ retains its dilute solution value because the rods are imagined to be infinitely thin:

$$D_\parallel = D_\parallel^0 \qquad D_\perp = 0 \tag{4}$$

From eq 2 it follows that:

$$D = \frac{1}{2}D^0 \tag{5}$$

The DE theory is an ideal model designed primarily to treat rotational diffusion and viscosity; even its promoters saw the difficulties with so simple a treatment of trans-

* To whom correspondence should be addressed.
® Abstract published in *Advance ACS Abstracts,* September 15, 1994.

0024-9297/94/2227-6871$04.50/0

lational diffusion.[26] Finite diameter, flexibility, hydrodynamic interactions, and the "decorrelating" effects[27] of Brownian bombardment by solvent were not considered. Yet these factors are unavoidable in real polymer solutions. Additionally, self-diffusion data for solvent-sized molecules in suspensions of rods[28,29] show that the very decrease of available space for diffusion as the rods become more concentrated results in reduced mobility that obviously has nothing to do with "entanglement". Finally, even if the 50% reduction in the diffusion coefficient predicted by eq 5 were correct, the transition to this condition is not described.

More advanced theories for the translational self-diffusion of rods include scaling[11,30] and perturbation approaches.[9,10,12-14] Scaling arguments have primarily addressed the flexibility issue. Semenov derived the dynamic structure factor for a single semiflexible probe molecule surrounded by invisible but otherwise identical molecules. The solution is considered to be concentrated when $(4Lp^2)^{-1} \ll \nu \ll (2Lpd)^{-1}$ where p is the persistence length in the Kratky-Porod wormlike chain model.[23,24] The self-diffusion coefficient,

$$D_s = D^0(p/(L + 2p)) \tag{6}$$

is identical to the DE prediction in the stiff limit ($L \ll p$). Since $D_\parallel{}^0 \sim L^{-1}$, the usual reptation result, $D \sim L^{-2}$, is obtained in the flexible limit. Tinland, Maret, and Rinaudo classify isotropic solutions as dilute, semidilute, and concentrated. In dilute solutions, the bending wormlike polymers obey standard continuum expressions.[7,22] In semidilute solutions, D_s scales according to:

$$D_s \sim p^{-5}L^{-2}c^{-3} \tag{7}$$

The concentration dependence in eq 7 is derived by introducing an intermolecular correlation length, ξ, as in the standard scaling argument for reptation in solutions.[31] For distances $\gg \xi$ a given chain can be described as a Gaussian sequence of "blobs" of size ξ. The number of chain segments inside a blob is obtained by replacing the usual monomer segment length with the Kuhn statistical segment length, $2p$. The requisite assumption for the chain to be well described by blobs in this way is that the blobs be large enough that real segments become decorrelated within them—i.e., $\xi \gg 2p$. Thus, application of eq 7 to solutions of very stiff chains may be inappropriate. In concentrated solutions, the theory of Tinland, Maret, and Rinaudo predicts a concentration-independent diffusion coefficient:

$$D_s = D^0p/L \tag{8}$$

The equation is meaningless in the stiff limit ($p = \infty$), but the concentration independence for ordinary values of p/L is interesting.

Green function/perturbation approaches were first applied to concentrated suspensions of rods by Edwards and Evans.[9] In their model, a rod of finite thickness diffuses through a tube, impeded occasionally by other rods, themselves imagined to be detained similarly. The process resembles linear diffusion through a series of gates that may open or close. The diffusion is predicted to obey

$$D_\parallel = \frac{3}{2}D^0(1 - C(\nu dL^2)^{3/2}) = \frac{3}{2}D^0(1 - \delta(\mathrm{v}/\mathrm{v}^*)^{3/2}) \approx \frac{3}{2}D^0\mathrm{e}^{-\delta(\nu/\nu^*)^{3/2}} \tag{9}$$

where C is a unitless constant of order unity and $\delta = C(16/\pi)^{3/2} \approx 11.5C$ according to eq 3. If $C = 1$, eq 9 predicts a "glass transition" or cessation of motion at $\nu dL^2 \approx 1$ or, equivalently, at $\nu/\nu^* \approx \pi/16 \approx 0.2$. Real rods at equilibrium remain fluid through the liquid crystal transition, so C must be small, such that the lyotropic transition preempts the glass transition. Glassing under nonequilibrium conditions has been considered as a possible gel mechanism[32] for rods. There is, however, no available evidence to suggest how closely the cessation of motion may be approached under any conditions of measurement.

Teraoka and Hayakawa adopted the Edwards-Evans approach to compute the decline of perpendicular diffusion with concentration, achieving the result[10]

$$D_\perp = D^0_\perp\,(1 + \epsilon\nu L^3)^{-2} \tag{10}$$

where ϵ is claimed to be a unitless constant. Using eqs 1-3 and introducing the axial ratio $x = L/d$, this can be rewritten as

$$D_\perp = \frac{3}{4}D^0(1 + \psi\nu/\nu^*)^{-2} \tag{11}$$

where

$$\psi = \epsilon\nu^*L^3 = (16\epsilon/\pi)x \tag{12}$$

In eqs 11 and 12 we have pushed the Teraoka-Hayakawa theory in a somewhat unnatural way, since their approach was really intended for thin rods. This anticipates the experimental results below, which will highlight the importance of finite thickness effects.

The Edwards-Evans theory for parallel diffusion was extended to a wider concentration range by Sato and Teramoto,[12] with the result:

$$D_\parallel = D_\parallel{}^0(1 - \alpha\nu dL^2)^2 \tag{13}$$

where α is a unitless constant. Equivalently, we may write

$$D_\parallel = \frac{3}{2}D^0(1 - \kappa\nu/\nu^*)^2 \tag{14}$$

where according to eq 3

$$\kappa = 16\alpha/\pi \tag{15}$$

To obtain the average diffusion coefficient, we combine eqs 11 and 14 according to eq 2:

$$D/D^0 = \frac{1}{2}[(1 - \kappa\nu/\nu^*)^2 + (1 + \psi\nu/\nu^*)^{-2}] \tag{16}$$

If the Edwards-Evans expression, eq 9, is used instead for $D_\parallel$, then:

$$D/D^0 = \frac{1}{2}[(1 - \delta(\nu/\nu^*)^{3/2}) + (1 + \psi\nu/\nu^*)^{-2}] \tag{17}$$

Experimental Section

Materials. The five PBLGs of different molecular weights purchased from Sigma will be referred to as PBLG-X where X is the vendor-supplied molecular weight. Labeled polymers will be referred to as LPBLG-Y, where Y is the measured molecular weight from static light scattering. Sample characteristics appear in Table 1.

Attachment of thiocyanate dyes at the terminal $-NH_2$ group of PBLG has been reported,[32-34] but the number of chain ends available, per unit mass of polymer, decreases with molecular weight. Also, the $-NH_2$ groups are not always present, due to reaction with various chemicals used during purification, forma-

Table 1. Characteristics of Labeled and Unlabeled PBLG in DMF and Pyridine

Sigma lot no.	M_w Sigma specified	[η] of unlabeled PBLG in DMF at 25 °C (dL/g)	[η] of unlabeled PBLG in pyridine at 25 °C (dL/g)	[η] of LPBLG in DMF at 25 °C (dL/g)	calcd no. of dyes/ polymer[a]	% of monomers dyed[a]	M_w of LPBLG by static light scattering	M_w/M_n from DLS/ Laplace inversion	length of LPBLG[b] (Å)	second virial coefficient A_2 of LPBLG in DMF (10^{-4} cm^3·mol·g^{-2})
Lightly Labeled (Scheme 1)										
96F-5049	26 000	0.105 ± 0.001		0.114 ± 0.001	0.7	0.8	20 000		137	4.39 ± 0.31
32H-5530	42 000	0.228 ± 0.001	0.233 ± 0.002	0.229 ± 0.001	1.1	0.6	36 000	1.2	246	3.59 ± 0.25
81H-5550	116 000	1.23 ± 0.02	1.33 ± 0.01	1.33 ± 0.01	5.0	0.9	103 000	<1.1	705	3.24 ± 0.23
85F-5020	260 000	2.72 ± 0.03	2.96 ± 0.06	2.83 ± 0.04	3.5	0.3	232 000	1.3	1590	2.29 ± 0.16
Heavily Labeled (Scheme 2, Supplementary Material)										
34F-5004	66 000	0.303 ± 0.003		0.698 ± 0.006	38	13	89 000		610	3.39 ± 0.24

[a] Maximum achievable from stoichiometry. [b] $L = (M_w/219)1.5$ Å.

Scheme 1

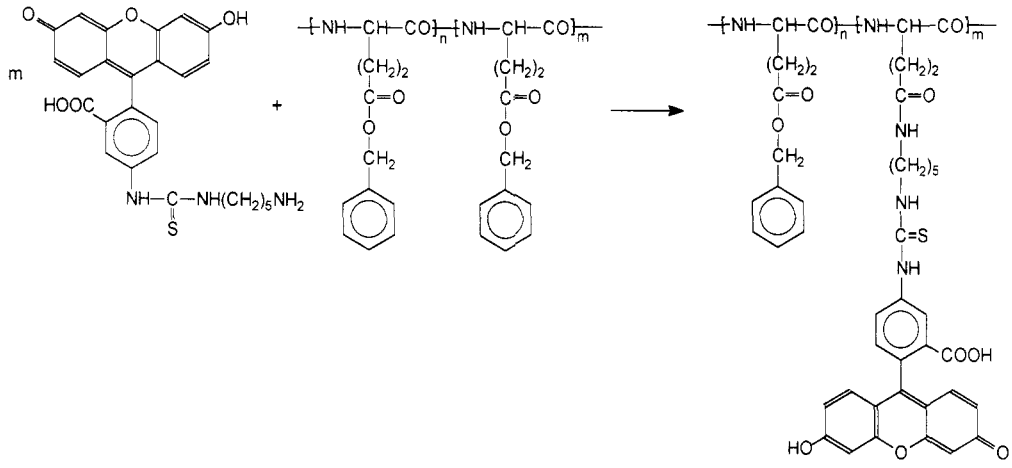

tion of unreactive pyrollidone rings, or coupling of chains.[35] For a recent review, see ref 36. In any case, end labeling of high molecular weight PBLG's as they normally come from the supplier was not effective. Side-chain substitution is the most reliable and flexible way to label PBLG. PBLG-26000, PBLG-42000, PBLG-116000, and PBLG-260000 were labeled with 5-[(5-aminopentyl)thioureidyl]fluorescein dye (fluorescein cadaverine; Molecular Probes Inc., Catalog No. A-456). Some of the side-chain benzyl groups along the backbone were replaced by the amine group on the dye as shown in Scheme 1. A typical recipe follows. One gram of PBLG was dissolved in 20 mL of pyridine. Fluorescein cadaverine dye was also dissolved in pyridine to make a ~3 mg/mL solution. The dye solution was added dropwise to the PBLG solutions under dry nitrogen at room temperature. The containers were wrapped with aluminum foil to isolate them from light, and the reactions were allowed to proceed for about 10 days under dry N_2. The reacted solutions were then concentrated by blowing filtered N_2 over them. The condensed solutions contained about 50–60% polymer; this would greatly reduce losses when precipitating the polymers from the solutions. The labeled PBLGs were precipitated out by adding water to the condensed solutions and enfolded in 0.1-μm polyethylene filter membrane (Nuclepore, SN:182105, Lot No. 83K2B20). Unreacted dye was first extracted by methanol in a Soxhlet extractor at about 60 °C for about 6 days. The polymer was then repeatedly dissolved in 20–30 mL of dioxane and reprecipitated with methanol until the rinse was no longer fluorescent when inspected in an epifluorescence microscope with 4880-Å illumination. The labeled PBLGs were vacuum dried at about 60 °C. In order to remove dust—important for DLS, not so for FPR—the polymers were redissolved in about 20 mL of tetrahydrofuran and centrifuged at 5000 rpm for 4 h. PBLGs were again concentrated by blowing a stream of filtered N_2 over the solutions and precipitated by adding water. The samples were vacuum dried and stored below 0 °C. Table 1 lists calculated stoichiometric ratios of dye to polymer for each sample. These represent maximum values, as the amide–ester exchange reaction is not quantitative. Various spectroscopic analyses were tried to estimate the actual dye content. It was too low for reliable estimation by NMR or IR, but visible absorption was somewhat successful. On the assumption that the attached fluorescein moiety has the same electronic absorption properties as free fluorescein dye dissolved in pyridine, an appreciable fraction of the macromolecules in the labeled preparations may have no bound dye. This may be especially true of the low-M samples.

LPBLG-89000 was prepared by a different scheme, resulting in a much higher dye content, increased molecular weight, and intrinsic viscosity. The method, which is described in the supplementary material, may cause cross-linking but might be useful if intensely bright polymers are desired. The significance of this heavily labeled polymer to the present study is that its behavior is qualitatively similar to the more lightly labeled samples prepared by Scheme 1.

PBLG solutions are critically sensitive to water (ref 37 and references therein). Solutions were made from fresh anhydrous pyridine (Aldrich; Catalog No. 27,097-0). Unused pyridine was stored in a desiccator and used later as the solvent for labeling other molecular weight PBLGs. The PBLG/pyridine solutions were prepared by weight and later converted into other concentration units using 0.791 mL/g for the partial specific volume of PBLG and 0.978 g/mL for the density of pyridine. The former value was measured for PBLG in DMF,[35,38] but the partial specific volume of PBLG is essentially independent of solvent, and also concentration, in helicogenic solvents.[38-40] The samples were made starting from the most concentrated solutions. After the FPR measurements had been finished at each concentration, solvent was added to the stock solution to make a more dilute solution. Dilute solutions were loaded in 0.2-mm-path-length rectangular microslides (Vitrodynamics) by capillarity; vacuum was applied when loading concentrated solutions. The microslides were flame-sealed. In samples more than several days old, moisture uptake through the occasional faulty seal sometimes resulted in a white gel phase, similar in appearance to the PBLG/DMF "complex phase",[37] near the meniscus. Samples were measured immediately after loading to avoid this problem, and the regions measured were far from the meniscus. The 0.2-mm cell thickness corresponds, for the largest labeled polymer, LPBLG-232000, to about 1300 rods laid end-to-end. Cell thickness effects were minor and will be considered later, in conjunction with the nonexponential recovery profiles seen at

high concentrations for one of the LPBLG samples.

Fluorescence Photobleaching Recovery. An intense laser beam briefly illuminates a coarse diffraction grating placed in the rear focal plane of an epifluorescence microscope to generate, by photobleaching, a square wave pattern of spacing L in the fluorescent sample. Then the grating is translated at a constant speed and projected into the sample by a less intense beam. As its image falls into and out of coincidence with the bleached pattern, a weak ac signal is produced, on top of a large dc base line from the unbleached fluorophores, at the anode of a photomultiplier tube that monitors the illuminated region. Initially, the ac signal resembles a triangle wave. As bleached and unbleached diffusers move about, the contrast of the bleached pattern is reduced. The ac signal loses its sharp edges and approaches a sine wave. The wave amplitude of the fundamental component decays at a rate, Γ, proportional to the diffusion coefficient of the fluorescent diffusers:[18] $ac(t) = ac(0) \exp(-\Gamma t)$, with $K = 2\pi/L$ and $\Gamma = DK^2$. The spatial frequency K may be varied by changing the coarse diffraction grating or the microscope objective. Bleach depths were less than 10% for all of the measurements, and it was usually possible to achieve this level of photobleaching with exposure times less than $0.1\Gamma^{-1}$, thus minimizing recovery during the photobleaching process. The decay rate Γ is obtained by fitting the wave amplitude of the fundamental to a single-exponential with floating base line, using a Marquardt nonlinear least-squares algorithm. Most of the samples were measured at several K values, and the diffusion coefficient and associated error were derived from the slope of a linear least-squares fit of the Γ vs K^2 plot. The precision was 2–5%. For a few of the very dilute samples, a single K value was used because the fluorescent intensity was weak for all but the highest power microscope objective (18×). The diffusion coefficient was calculated as $D_s = \Gamma/K^2$, and several repeat runs were made. Typical precision for these few measurements was ~12%. Further details of the FPR instrument, which is conceptually similar to that of Lanni and Ware,[18] have appeared elsewhere.[41] All FPR measurements were at 25.0 ± 0.2 °C.

Light Scattering Measurements. All five of the labeled PBLGs were measured by static light scattering in anhydrous *N,N'*-dimethylformamide, DMF (Aldrich; Catalog No. 22,705-6), since scattering by PBLG in pyridine is weak. The DMF was filtered through a 0.2-μm Acrodisc poly(tetrafluoroethylene) (PTFE) syringe filter (Gelman; Catalog No. 4225) under Ar. The labeled polymers were dissolved in the filtered DMF to make stock solutions and centrifuged at 7000*g* for 18–24 h to remove dust. The solutions were topped with Ar and sealed with PTFE screw caps. Since the polymers were fluorescent, static light scattering experiments were performed using the red light of a 6328-Å helium–neon laser (Spectra-Physics SP-124b, ca. 20 mW). The specific refractive index increment dn/dc at $\lambda_0 = 6328$ Å was taken[42] as 0.118 ± 0.004 mL/g. The light labeling and use of a wavelength far removed from the main absorption maximum should ensure that this value is approximately correct for LPBLG. All light scattering measurements were at 40.0 ± 0.2 °C. Dynamic light scattering measurements were performed in the same cells and in the same instrument[42,43] but not simultaneously. Optical settings in the detector were separately optimized for dynamic and static measurements.

Intrinsic Viscosity Measurement. To investigate changes on labeling, intrinsic viscosities of all five unlabeled and labeled PBLGs were measured in DMF using an Ubbelohde viscosimeter under dry N_2. The intrinsic viscosities of unlabeled PBLG-116000, PBLG-260000, and PBLG-42000 were also measured in pyridine under similar conditions to investigate differences between DMF and pyridine as solvents. The measurements were at 25.0 ± 0.2 °C. As the solvent flow time was about 240 s, the kinetic energy correction was not made.

Polymer Characterization

FPR is less susceptible than many other diffusion techniques to ambiguities in data interpretation, and sample preparation is completely trivial once the polymer is labeled. However, these important conveniences are not without a price. Fluorescein-based dyes, chosen for the seemingly complete irreversibility of their photobleaching, were strongly quenched in dry DMF, the most commonly used good solvent for PBLG. Of the very few good solvents that support unaggregated PBLG helices,[44] only in pyridine did fluorescein-based dyes glow brightly and yet undergo photobleaching upon application of acceptably short laser pulses. Pyridine is known to be a "good" solvent for PBLG,[39,44] but thermodynamic details are less abundant than for PBLG/DMF.[42,45] As PBLG scatters only weakly in pyridine, this information is not directly available from light scattering. In addition to establishing the solvation qualities of pyridine, it must be shown that the fluorescent labels do not perturb the PBLG structure. Then, absolute molecular weights and polydispersities of the labeled polymers must be measured without interference from the dye moiety. A combination of computer simulation, viscosimetry, light scattering (in DMF), and polarizing microscopy was used to address these issues. Except for computer simulation, these tests measure all the molecules in the labeled preparation and are less effective for lightly labeled preparations. FPR measurements and fluorescence microscopy observations provided additional support specific to those molecules in the labeled preparation that actually have dye substituents attached.

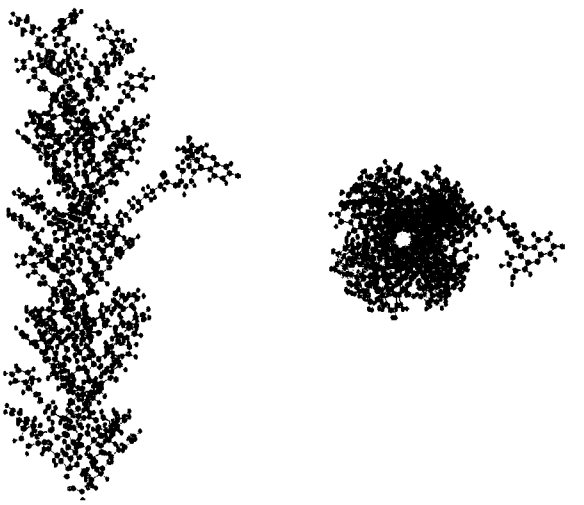

Figure 1. SYBYL structures for LPBLG labeled according to Scheme 1 to show how far dye projects. The right view is looking down the helix axis.

Prior to the synthetic effort, the program SYBYL (Tripos Associates) was used to assess possible structural alterations due to dye attachment. A weak perturbation was observed only in the experimentally unlikely case that two dyes were attached to adjacent PBLG repeat units. This result is consistent with the expectation that labeling would be fairly benign, since the dye substitution occurs far from the helix backbone and since the bulky dye moiety is attached through the relatively long $-NH(CH_2)_5-NHCSNH$ spacer (see Scheme 1). These encouraging simulations were useful for qualitative visualization of the labeled structure (Figure 1), but they do not constitute a comprehensive study and would not be conclusive in any case, since solvent was not included.

The intrinsic viscosity $[\eta]$ is sensitive to small structural perturbations and aggregation. The data appearing in Tables 1 and 2, and in the Mark–Houwink plot (Figure 2) establish that intrinsic viscosities in DMF are not greatly affected by the labeling procedure. The exception is LPBLG-89000, where the heavy labeling (by a different method than shown in Scheme 1; see supplementary information) resulted in intrinsic viscosity and measured molecular weight significantly higher than specified by

Table 2. A Points and Critical Concentrations

M_w	L/Å	w_A (%)	c_A (g·mL^{-1})	ϕ_A	ν_A (10^{17} mL^{-1})	ν^* calcd[a] (10^{17} mL^{-1})
20 000	137	33.4	0.353	0.279	106	170
36 000	246	20.8	0.214	0.170	35.8	52
103 000	705	12.3	0.124	0.0980	7.24	6.4
232 000	1590	11.7	0.118	0.0932	3.06	1.3

[a] Computed using d = 16 Å.

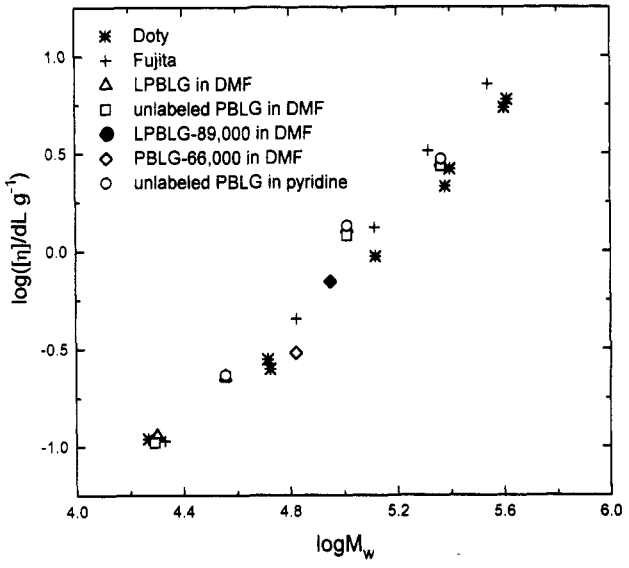

Figure 2. Mark–Houwink plots for labeled and unlabeled PBLG and LPBLG in DMF and pyridine (see text).

the manufacturer for the unlabeled material. Diffusion results for LPBLG-89000 are included because they show that the fundamental character of diffusion is not greatly affected even by very heavy labeling. Nevertheless, LPBLG-89000 data are not used to establish any trends regarding diffusion at high concentrations. The intrinsic viscosities of the other labeled polymers were, on average, 5% higher than those of the unlabeled materials. This difference exceeds the very small uncertainties quoted in Table 1, which are derived from the standard errors in the linear least-squares analysis used to obtain the intrinsic viscosity from the usual plots. Systematic error (a few percent) is not reflected in the tabulated uncertainties. There would be some cause for concern had the intrinsic viscosities of labeled materials been lower than those of the unlabeled materials, since this would imply kinking or bending of the helix. We can think of no good reason for the slightly higher intrinsic viscosities for the labeled materials. However, the effect is small. The Mark–Houwink exponents (from $[\eta] = K'M_w^a$) were $a = 1.35 \pm 0.08$ and 1.36 ± 0.097 for PBLG and LPBLG in DMF, respectively (omitting PBLG-66000 and LPBLG-89000). The K' value was 6.8 ± 0.4 dL/g for both labeled and unlabeled polymers in DMF. These virtually identical Mark–Houwink values are in good agreement with the results reported by Doty[46] many years ago for PBLG in DMF (the values $a = 1.33 \pm 0.07$ and $K' = 6.8 \pm 0.4$ dL/g are obtained by fitting their data). All the intrinsic viscosity data demonstrate that PBLG is not a perfectly rigid rod because $a < 1.8$. Solvent effects were very minor: the intrinsic viscosities of unlabeled PBLG-42000, PBLG-116000, and PBLG-260000 were 4–7% higher in pyridine than in DMF. Mark–Houwink parameters in pyridine were 1.38 ± 0.2 and 6.9 ± 0.9—i.e., within error of the parameters in DMF.

The argument against any deleterious effects of Scheme 1 dye labeling is not yet airtight. As $[\eta]$ of LPBLG in pyridine was not measured, due to the precious nature of the labeled material, the possibility that *labeled polymer* behaves differently in pyridine than in DMF is not rigorously excluded. Given the light labeling, this seems extremely unlikely. Temperature-dependent FPR studies showed no sign of LPBLG aggregation in pyridine, attesting to the absence of dye-induced (or water-induced) aggregation. Further evidence comes from polarizing microscope observations of the volume fraction at which the liquid crystal phase first appears, or Flory A point, ϕ_A. The A points in Table 2 for LPBLG/pyridine closely match the literature values[47] for PBLG in DMF; see Figure 3. The A points in either DMF or pyridine exceed those for PBLG in the aggregating solvent, dioxane.[48] This is evidence that LPBLG/pyridine solutions are virtually identical to PBLG/DMF solutions at any concentration in the isotropic regime of interest. Indeed, we believe pyridine to be a better solvent than DMF based on direct comparison of the quantity of added water required to induce PBLG precipitation in both solvents. PBLG/DMF has been shown conclusively not to undergo aggregation in the usual sense, as its osmotic modulus remains positive nearly to the A point.[42] Formally transient but decidedly long-term "pretransitional" structures[49,50] of ill-defined nature develop in concentrated solutions of PBLG/DMF and, presumably, in PBLG/pyridine. These pretransitional structures may be due to critically slowed coupling between orientational and translational order parameters as the liquid crystalline boundary is neared. However, such transient structures do not constitute aggregates. At low axial ratios, the observed A points are closer to the Onsager expectation[51] ($\phi_A = 4/x$) than to that of Flory[52–54] ($\phi_A = (8/x)(1 - 2/x)$). Leveling of ϕ_A at a value higher than the Onsager prediction occurs for $x > \approx 50$, corresponding to $L \approx 800$ Å. This is a reasonable estimate of the PBLG persistence length.[55–57]

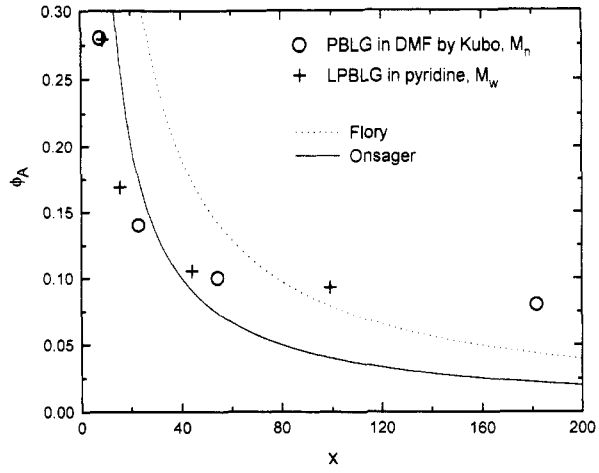

Figure 3. Onset of liquid crystal transition at volume fraction ϕ_A which is similar for LPBLG/pyridine and PBLG/DMF. Flory[54] and Onsager[51] predicted curves are provided for reference. In this figure only, the thermodynamic diameter of 16 Å was assumed for the purpose of computing the axial ratio.

Light scattering measurements of LPBLG's were straightforward, except that a weak HeNe laser operating at $\lambda_0 = 6328$ Å was required to avoid photodegradation, thermal lensing, and fluorescence corrections that would depend on the exposure time in the beam. As shown in Table 1, the weight-average molecular weights, M_w, of the labeled polymers are in good agreement with the manufacturer-supplied data for the unlabeled material except, as already mentioned, for the specially prepared and heavily labeled LPBLG-89000. To assess polydispersity, intensity autocorrelation functions were obtained at low

Table 3. Zero Concentration Diffusion Coefficients for LPBLG from FPR and DLS for Pyridine at 25 °C (All: 10^{-7} cm²/s)

M_w	D^0_{FPR}	D^0_{DLS}[a]
	Lightly Labeled	
20 000	8.77 ± 0.16	8.40 ± 0.13
36 000	4.44 ± 0.18	4.97 ± 0.13
103 000	2.44 ± 0.02	2.28 ± 0.03
232 000	1.46 ± 0.03	1.50 ± 0.01
	Heavily Labeled	
89 000	3.62 ± 0.08	

[a] Data obtained in DMF at 40 °C and corrected using $\eta_0 = 0.00884$ g/(cm·s) for pyridine at 25 °C and $\eta_0 = 0.00680$ g/(cm·s) for DMF at 40 °C.

values of qL ($q = 4\pi n \sin(\theta/2)/\lambda_0$ where n is the refractive index of DMF, 1.43, and θ is the scattering angle) to avoid interference from the end-over-end rotational term.[58] Due to polydispersity, the electric field autocorrelation function will be represented approximately by $g^{(1)}(\tau) = \Sigma A_i \exp(-\gamma_i\tau) \approx \int d\gamma\ A(\gamma) \exp(-\gamma\tau)$ where A_i is the scattering amplitude for the ith component, proportional to weight/volume concentration and molecular weight, modified by the particle form factor, a function of the product of q and L: $A_i = c_i M_i P(qL_i)$. The decay rate γ_i is related to molecular weight via the diffusion coefficient, $\gamma_i = q^2 D_i$, where the D vs M relationship for PBLG in DMF at 40 °C is[58] $D/(\text{cm}^2\,\text{s}^{-1}) = (2.75 \pm 1.7) \times 10^{-3} M^{-0.78\pm0.05}$. Thus, the c vs M distribution can be obtained. It was found to be unimodal for all the labeled polymers. The measured distribution is probably a little broader than the actual one, since CONTIN does not return a single exponential even for a purely monodisperse sample. Even so, the ratio of weight- to number-average molecular weights, M_w/M_n, remained <1.3 for all the samples (Table 1). An even narrower distribution would be desirable for testing some aspects of the Doi–Edwards theory, especially rotational diffusion and viscosity where very strong power law dependencies are predicted. Nevertheless, the distributions of the labeled polymers are adequately narrow for the present purpose.

The z-average[59] diffusion coefficients from DLS in DMF at 40 °C, extrapolated to zero concentration, were in good agreement with appropriate hydrodynamic continuum expressions[7,22] computed for monodisperse polymers with $M = M_w$. In Table 3 and Figure 4, the DLS diffusion coefficients have been adjusted for temperature and viscosity, so that they may be compared to those from FPR. As shown, the self-diffusion values extrapolated to infinite dilution are in close agreement with the DLS results and with the hydrodynamic expressions. The differences are only a little bit outside the estimated uncertainties, and there is no trend. This is very significant, because in all the previously described intrinsic viscosity, light scattering, and phase behavior tests favoring the benign effects of labeling, *all* the polymers in the labeled population contributed to the measured property. These tests could have failed to detect damaged polymers if labeling were so light that a significant portion of the chains remained unlabeled, as is possibly the case for LPBLG-20000 and LPBLG-36000. The good agreement between FPR (representing just the labeled polymers in the labeled preparation) and DLS (representing all polymers in the labeled preparation) indicates labeling causes no serious structural perturbation, at least none that is observed in dilute solution. It is still desirable to display, while observing only the labeled polymers in any given preparation, that there is no serious alteration of properties in concentrated solution. To do this, PBLG-260000 and LPBLG-232000 were mixed approximately equally by weight and diluted with pyridine until the narrow biphasic regime was entered. The biphasic solution consists of a dispersion of liquid crystalline and isotropic domains of almost equal concentration.[48] The former appear bright between crossed polars of the microscope and the latter dark. Using epifluorescence microscopy, it was observed that the labeled polymer molecules entered both phases essentially equally. Had the labeled polymer been seriously perturbed, it would have been excluded preferentially from the liquid crystalline phase.[54] In summary, whether one looks at all the molecules in a labeled preparation or just those that are actually labeled and whether one looks at dilute solution properties or phenomena associated with the liquid crystalline transition, there is no evidence for altered solution properties by side-chain labeling.

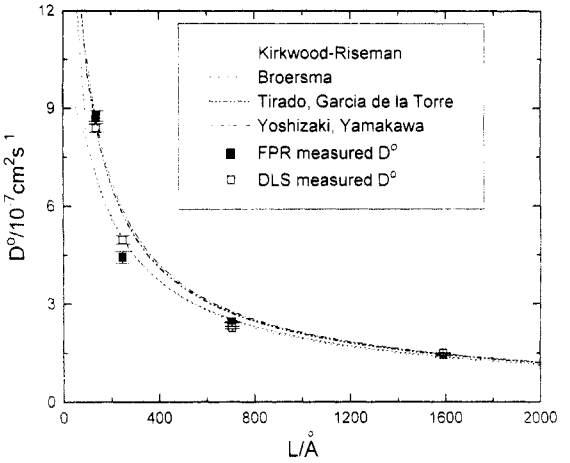

Figure 4. D^0 from DLS (open squares) and FPR (full squares) in agreement with each other and also in reasonably good agreement with appropriate hydrodynamic theories. Lower two curves: Broersma and Kirkwood–Riseman equations. Upper two curves: Tirado et al. and Yoshizaki and Yamakawa curves. All curves were computed with the hydrodynamic diameter 20 Å. See also Table 2.

The Question of Diameter

In the hydrodynamic expressions, a value for d must be assumed. There is no reason to expect this to be identical to the value from thermodynamic measurements (d = 16 Å[42]) because PBLG is not a smooth cylinder. We used d = 20 Å to compute the various hydrodynamic continuum values in Figure 4. The same value is used elsewhere in this paper to normalize number densities (i.e., to compute νdL^2 and ν/ν^*). In previous combined static and dynamic light scattering work,[42] we used d = 16 Å because of the role of thermodynamics in the measured mutual diffusion. In the present paper, we use d = 16 Å only for Figure 3 and Table 2 which concern purely thermodynamic behavior.

Diffusion as a Function of Concentration

Figure 5a shows an FPR trace for ca. 29% LPBLG-20000/pyridine. Despite the high concentration, near the lyotropic liquid crystalline boundary, only a little nonexponentiality is evident. Nonexponentiality is somewhat more pronounced in Figure 5b which shows a ca. 10% LPBLG-232000 solution, also near its lyotropic transition point. Despite this worst-case nonexponentiality, single-exponential fits with a floating base line were well behaved for this sample and all others in the isotropic regime. The average decay rate always scaled nicely with K^2 as shown in the inset, with zero intercepts to confirm the absence of chemical recovery of the dye. The main self-diffusion results (supplementary material) can be viewed from many different perspectives. We show only a few.

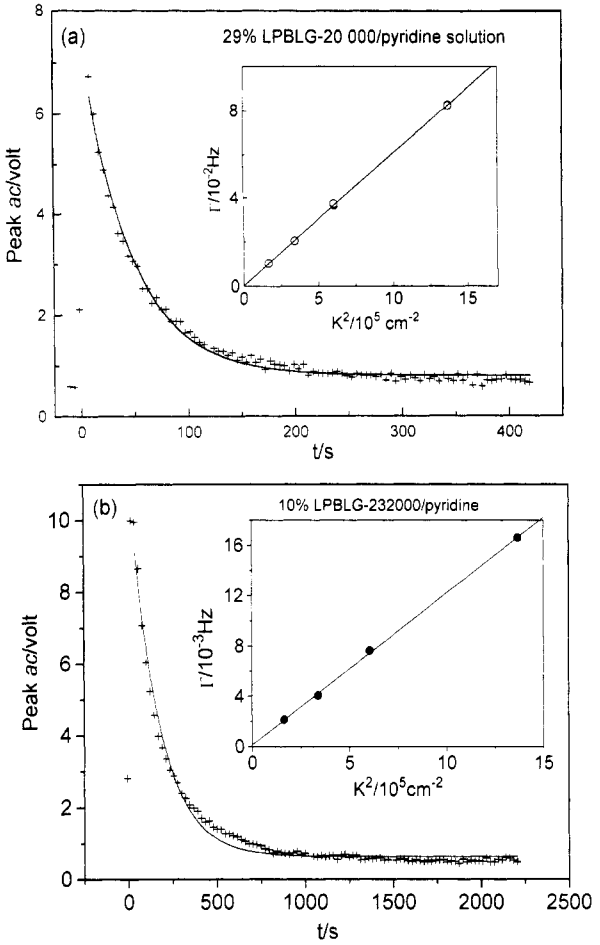

Figure 5. (a) Recovery for 29% LPBLG-20000 which is very slightly nonexponential. At lower concentrations, nonexponentiality would be still less. (b) Worst-case nonexponentiality for ca. 10% LPBLG-232000. Insets: recovery rates depend linearly on squared spatial frequency despite nonexponentiality; the intercept is zero within error.

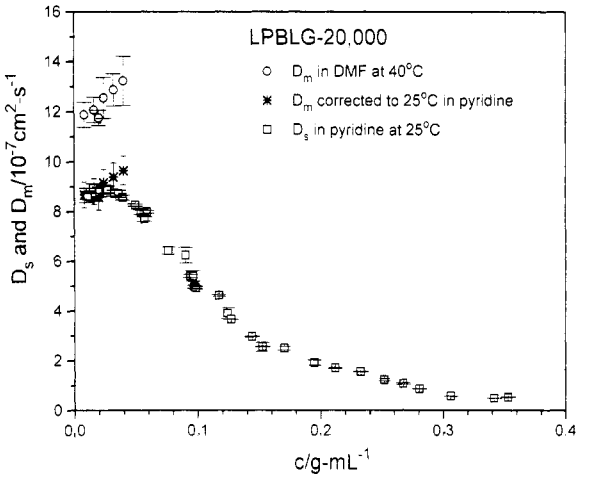

Figure 6. Mutual diffusion and self-diffusion coefficients from DLS and FPR respectively for LPBLG-20000. The DLS data were obtained in DMF at 40 °C (open circles) and corrected to pyridine at 25 °C (*) for comparison to the FPR data (open squares).

Figure 6 combines mutual diffusion, D_m, with self-diffusion, D_s, for LPBLG-20000. Under the labeling conditions employed here, the average diffusion coefficient from FPR would be a weight average.[41] The close agreement between the weight-averaged D_s from FPR and the z-averaged D_m from DLS, and the agreement of either with hydrodynamic models, suggests low or moderate polydispersity for the labeled samples. D_s decreases while

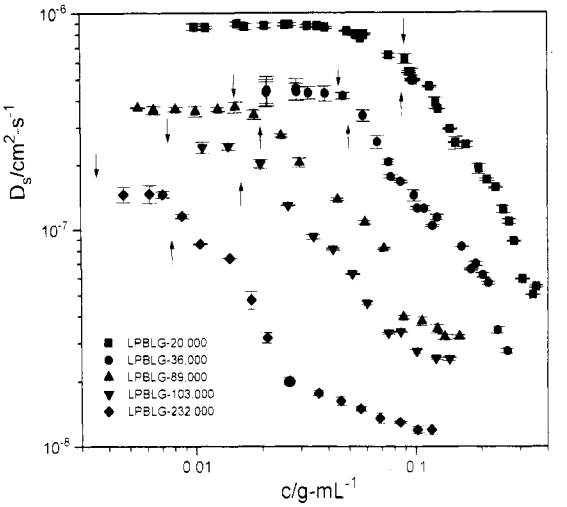

Figure 7. Concentration dependence of D_s for LPBLG-20000 (filled squares), LPBLG-36000 (filled circles), LPBLG-89000 (filled up triangles); LPBLG-103000 (filled down triangles), and LPBLG-232000 (filled diamonds). Errors are often smaller than the data points. Up arrows denote the condition $\nu dL^2 = 1$. Down arrows show the condition $c = [\eta]^{-1}$.

Table 4. Crossover Concentrations When D_s Starts To Decrease

	$1/[\eta]$ (g mL^{-1})	c^+ from FPR (g mL^{-1})	ν^+L^3	ν^+dL^2 [a]	ν^+/ν^{*a}
20 000	0.088	0.076	6	0.86	0.17
36 000	0.044	0.043	10	0.87	0.17
103 000	0.008	0.017	40	0.99	0.19
232 000	0.004	0.007	75	0.92	0.18
89 000*	0.014	0.018	28	0.91	0.18

[a] Using d = 20 Å. * = heavily labeled material.

D_m increases, as expected from previous studies.[42,60-63] A level (or slightly decreasing) behavior has been reported[43,62] for D_m vs c in PBLG/DMF. This behavior is not pronounced here, possibly because the uncertainties are too large. As a result, the D_m values could be very slightly underestimated; agreement of D_m and D_s at low concentrations was within 10% for all the labeled samples. The zero concentration diffusion coefficient, D^0, from FPR (Table 3) scales as $M^{-\beta}$ with $\beta = 0.7 \pm 0.1$. This is within error of the DLS result for PBLG,[43,57] $\beta = 0.78 \pm 0.05$, and both values are significantly different from the expectation in a long, rigid limit ($\beta = 1$). At concentrations exceeding 30 mg/mL, β from FPR approximately doubles.[64]

The self-diffusion results are collected in Figure 7. For all molecular weights, D_s is level at low concentrations and exhibits a fairly sharp downturn at a concentration c^+. Values for c^+ were estimated graphically as the intersections of lines drawn through the dilute, level regimes and lines drawn through the strongly decreasing regimes from log–log plots. As shown in Table 4, c^+ greatly exceeds the concentration at which $\nu L^3 = 1$. This is true for all molecular weights. A better estimator is $c^+ \approx [\eta]^{-1}$, but Figure 8 shows that c^+ systematically exceeds $[\eta]^{-1}$ for the higher molecular weights. While $[\eta] \sim M^{1.35}$, the downturn concentration exhibits less M-dependence: $c^+ \sim M^{-0.96\pm0.03}$. Considering that $\nu = cN_a/M$, where N_a is Avogadro's number, and since $M \sim L$, we find that $\nu^+ \sim L^{-2}$ within uncertainty. In fact, c^+ corresponds closely to the condition $\nu dL^2 \approx 1$ or, equivalently, to $\nu/\nu^* \approx 0.2$. This corresponds approximately to a number density of $1/A_{2,\nu}$ where $A_{2,\nu}$ is the osmotic second virial coefficient[51] with concentration expressed as number density: $A_{2,\nu} = \pi dL^2/4$. Closer inspection reveals that the lowest-M polymer approaches the downturn somewhat more gradually. The

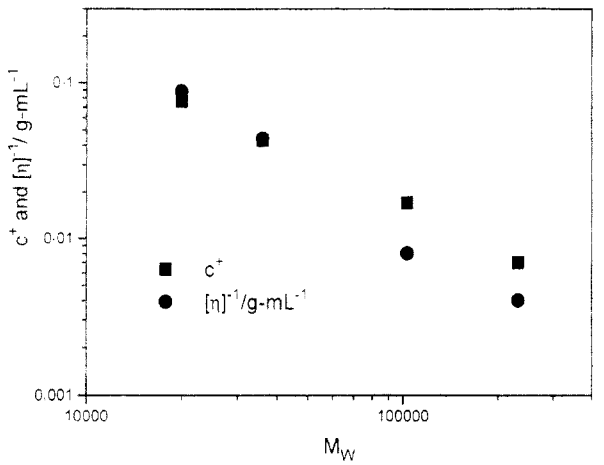

Figure 8. Downturn concentration and inverse intrinsic viscosity against molecular weight.

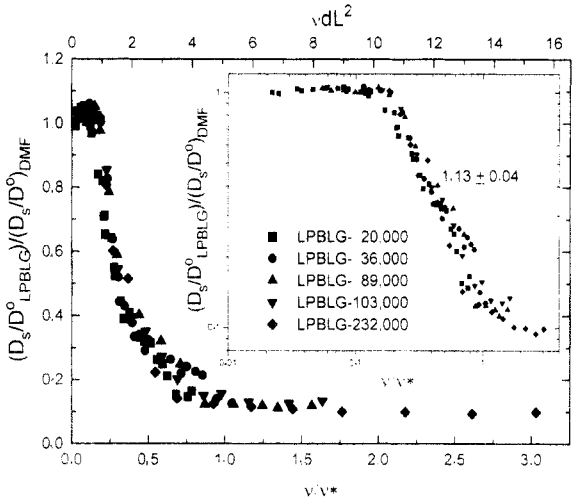

Figure 9. Near collapse of the data in Figure 7 to a single curve in a linear axis representation. Data have been scaled by D^0 and by the diffusion of solvent (pyridine) estimated from available data for DMF. Inset: log–log representation. Symbols: same as Figure 7.

first sign of downturn for this smallest polymer corresponds to $\nu/\nu^* \approx 0.1$, or $\nu dL^2 \approx 0.5$. In evaluating these results, it must be remembered that only one value of d has been tested. Thus, we *do not* claim $\nu^+ \sim d^{-1}$, a scaling relation that would clearly behave very badly at $d = 0$. Also, the condition $\nu^+ dL^2 \approx 1$ could be coincidental or specific to the particular range of axial ratios investigated ($7 < x < 80$).

The similar appearance of the curves in Figure 7 suggests that the data might be scaled. The most successful attempt appears in Figure 9 where the number density is scaled to ν^* computed from eq 3 (using $d = 20$ Å and $L = 1.5 \times (M_w/219)$ Å where 1.5 Å is the monomer translation length along the helix and 219 the monomer molecular weight). The diffusion data are scaled by the dilute solution value, D^0, and also by the ratio D/D^0 for solvent, estimated from the available DMF diffusion data obtained by pulsed field gradient NMR.[28,29] The solvent diffusion term has only a minor effect, since solvent mobility in PBLG is governed effectively by the decrease in volume fraction available for diffusion and since very significant volume fractions in the isotropic phase can only be reached for the shortest polymer. If the solvent diffusion term is left out, only the smallest sample (LPBLG-20000) is appreciably affected and it then matches the other data a little better in the dilute regime ($\nu/\nu^* < 0.1$) but droops to about 0.05 instead of leveling near 0.1 as ν^* is approached. With or without the solvent diffusion correction, the near collapse to a single curve in a linear plot, with no adjustable parameters, is remarkable. Scaling the number density by L^3 instead of ν^* does not produce such universality.[64] A second, slowly decreasing regime seems to appear above $\nu/\nu^* \approx 1$, but most of the points are for the largest, most flexible sample whose isotropic phase extended to above the critical point predicted for a rod.

The inset to Figure 9 shows the log–log representation. The power law in the strongly decreasing region ($0.19 < \nu/\nu^* < 0.94$) is $(D_s/D^0)_{LPBLG}/(D_s/D^0)_{solvent} \sim (\nu dL^2)^{-1.13\pm0.04}$. As mentioned already, we find $D^0 \sim L^{-0.7}$. Since $\nu = cN_a/M_w$ and since the solvent term is minor, we obtain $D_s \sim c^{-1.13\pm0.04}L^{-1.8\pm0.2}$.

Discussion

No theory matches the observed behavior exactly. The simple DE approach with its prediction that $D/D^0 = {}^1/_2$ for $\nu L^3 > 1$ is clearly inadequate, as expected for the reasons mentioned earlier. The extension to flexible coils by Semenov[11] suffers mostly the same problems, and the present, weakly bending samples are inappropriate to test this theory. The scaling approach of Tinland, Maret, and Rinaudo[30] is of questionable validity if excluded-volume (finite thickness) effects are significant. It does successfully predict that three regimes will be observed—concentration-independent behavior at low and high concentrations, connected by a strongly decreasing zone. However, the predicted c^{-3} dependence in the intermediate regime is much stronger than the observed $c^{-1.13}$. The observed $L^{-1.8}$ behavior is only a bit lower than the reptation-like L^2 dependence predicted for random coils; see eq 7.

The Green function approaches, eqs 16 and 17,[9,10,12] do not match the data well at low and high concentrations. The equations below maintain the same general form but provide "offsets" along both the concentration and diffusion axes:

$$D/D^0 = b + {}^1/_2[(1 - \kappa(\nu/\nu^* - \nu^+/\nu^*))^2 + (1 + \psi(\nu/\nu^* - \nu^+/\nu^*))^{-2}] \quad (16')$$

$$D/D^0 = b + {}^1/_2[(1 - \delta(\nu/\nu^* - \nu^+/\nu^*)^{3/2}) + (1 + \psi(\nu/\nu^* - \nu^+/\nu^*))^{-2}] \quad (17')$$

Here, b is the "base line" diffusion rate (about 0.1 from Figure 9) and ν^+ is the number density at c^+ ($\nu^+/\nu^* \approx 0.1$–0.2, according to the discussion surrounding Figure 7). These two equations were fitted to the D/D^0 vs ν/ν^* curve at each molecular weight. As already mentioned, the Teraoka–Hayakawa formalism was not intended for rods of finite diameter. Still, one can test for the mark of success of the functional forms suggested by these Green function/perturbation approaches, which would be a fitted ψ scaling linearly with $x = L/d$ (see eq 12). In performing the nonlinear least-squares fits, only points satisfying $\sim 0.15 < \nu/\nu^* < \sim 1$ were used. Several initial guesses were tried to guard against false minima. The analysis was performed with and without the solvent correction term $(D/D^0)_{DMF}$, which made little difference, especially for the higher mass LPBLG's whose isotropic phase includes only low volume fractions. The analysis was also repeated with parameter b allowed to float or fixed at 0.1. Equation 17′ was able to fit the data very well when b was allowed to vary, but the Marquardt nonlinear least-squares algorithm [Microcal Origin, version 3.0] returned unrealistic, negative values of b and ψ. Equation 17′ did not fit the data well when parameter b was fixed. Equation 16′ has the

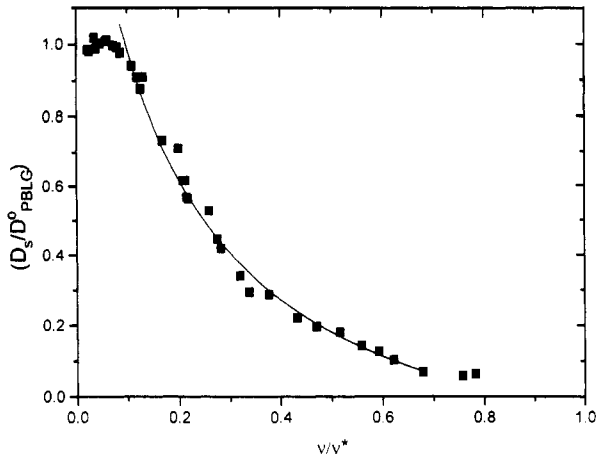

Figure 10. Sample fit to reduced diffusion data, using eq 16′ for LPBLG-20000.

Table 5. Parameters of Fit to $(D/D^0)_{LPBLG}/(D/D^0)_{DMF}$ for Equation 16′

	$\kappa(\|)^a$	$\psi(\perp)^a$	ν^+/ν^{*a}	b^b
LPBLG-20000	1.7 ± 0.3	2.5 ± 1	0.09 ± 0.01	0.10 ± 0.04
LPBLG-36000	1.3 ± 0.3	12 ± 6	0.16 ● 0.02	0.14 ● 0.03
LPGLG-103000	1.3 ± 0.2	3.6 ● 1.5	0.14 ± 0.01	0.06 ± 0.09
LPBLG-232000	1.3 ± 0.1	8.0 ● 2.5	0.17 ± 0.01	0.08 ± 0.03

[a] Uncertainty reflects the difference between fitting all four parameters simultaneously and holding b at 0.1, or the estimate from the error matrix, when larger. [b] Uncertainty comes from the error matrix when fitting all four parameters simultaneously.

unrealistic characteristic that D increases at $\nu > \nu^*$. Even so, it was generally more successful than eq 17′ as it did not produce unphysical values of b and ψ. An example is shown in Figure 10, and other results are compiled in Table 5. On the main point of how ψ scales with the axial ratio, the large uncertainties for this parameter render the analysis inconclusive. A qualitative feel for the size of the parameters in the Green function/perturbation approaches is all that can be claimed. The remarkable result is that the term describing the reduction in diffusion perpendicular to the rods (ψ) is larger, but not very much larger, than the term describing the decrease in parallel motion (κ). The reduction in mobility due to loss of perpendicular motion, the topological constraint expected after νL^3 exceeds unity, is greatly delayed. By the time it matters, the effect of finite diameter becomes almost as important, and the reduction in diffusion with concentration seems to occur more or less in one step. If the data of Figure 7 are replotted with a linear ordinate scale, there is a hint of a two-stage rolloff in diffusion for the two highest molecular weights (indeed, the effect is just barely visible in the log–log representation for the highest molecular weight). Perhaps with very stiff samples at very high axial ratios, the loss of transverse motion due to topological constraints could be well separated from rod-jamming effects due to finite thickness.

If comparison to theory is difficult, the phenomenology is remarkably simple. In addition to the power law result already quoted ($D_s \sim c^{-1.13\pm0.04}L^{-1.8\pm0.2}$), the merged data sets for all molecular weights are well fit, at concentrations above the dilute regime, by a simple exponential:

$$(D_s/D^0)_{LPBLG}/(D_s/D^0)_{DMF} = b + a\exp(-\alpha'(\nu/\nu^* - \nu^+/\nu^*))$$

where $a = 0.91 \pm 0.01$, $b = 0.12 \pm 0.02$, $\alpha' = 0.20 \pm 0.01$, and $\nu^+/\nu^* = 0.15 \pm 0.01$. If the solvent diffusion term is left out, the results are somewhat sensitive to which low-c points are omitted since convergence of the LPBLG-20000

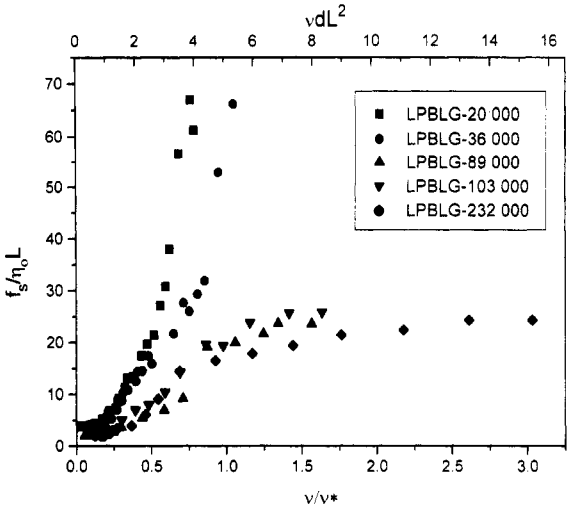

Figure 11. Self-friction, scaled by solvent viscosity and rod length, which is initially level and then begins to increase with concentration at $\nu/\nu^* \approx 0.1$–0.2.

data is not quite as good in the beginning of the strongly decreasing regime. We estimate $a \approx 1.1$, $b = 0.10 \pm 0.01$, $\alpha' \approx 0.17$, and $\nu^+/\nu^* \approx 0.12$.

Comparison to computer simulations poses interesting questions. Of several available studies (refs 27, 65, and 66 and references therein), the Brownian dynamics approach of Bitsanis, Davis, and Tirrell (BDT) seems particularly relevant.[27] These authors obtained parallel, perpendicular, and rotational diffusion for rods of axial ratio $x = 50$ in the semidilute regime. It was shown previously (ref 42, figure 21) that the BDT result for the average self-diffusivity, $D_{s,BDT}$, was in close agreement with the diffusion-like quantity kT/f_m where f_m, the mutual friction factor per rod for cooperative motion as in response to a concentration gradient, is obtained by combined static and dynamic light scattering experiments (SLS/DLS). Since $D_s = kT/f_s$, where f_s is the friction factor for motion of a single molecule, the agreement between $D_{s,BDT}$ and kT/f_m suggested that $f_s \approx f_m$. On this basis, the rapid rise of f_m with concentration[42] and initially level or slightly decreasing D_m vs c behavior[43,62] were tentatively associated with the loss of motions perpendicular to the rod axes. However, one should not generally expect f_s and f_m to be the same. In ref 42, great care was taken not to confuse the quantity kT/f_m with D_s, although kT/f_m is clearly closer to D_s than is D_m (at least kT/f_m decreases with concentration). At the outset of the present FPR study, given the close agreement between the BDT simulation and kT/f_m, we expected to find that $f_s \approx f_m$ and thus validate combined static and dynamic light scattering as a method to investigate the motion of individual rods. We now show that this is simply not the case; DLS cannot provide information about individual rods, even when combined with static light scattering results to isolate a (mutual) friction coefficient. This is not an indictment of SLS/DLS. FPR and other self-diffusion techniques are equally inept at providing information on collective particle motions which are important in many practical applications. Complete characterization of the system requires both f_s and f_m to be known.

Figure 11 shows f_s from the FPR measurements, scaled to a unitless parameter by the solvent viscosity, η_0, and rod length. Effectively, the plot shows the friction per unit rod length—or "intrinsic" friction. The analogous plot for f_m appears in Figure 9 of ref 42. There are some similarities. The intrinsic friction is higher for short rods than for long ones, whether f_s or f_m is considered. For the

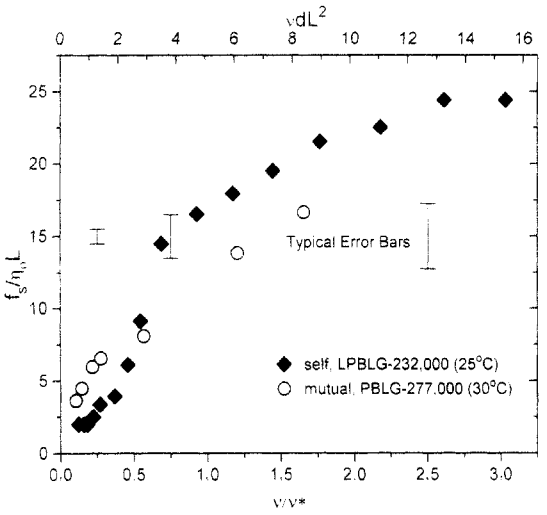

Figure 12. Mutual friction factor for PBLG-277000 (open circles)[42] and self-friction factor for LPBLG-232000 (filled diamonds).

longer PBLG or LPBLG samples at high concentrations, the scaled f_m and f_s each flatten. Both observations are probably the result of flexibility. The differences between f_s and f_m are also notable. The intrinsic self-friction is independent of concentration at low concentrations, while $f_m/\eta_0 L$ increases immediately with concentration. Figure 12 compares f_m for PBLG-277000 of ref 42 and f_s for LPBLG-232000. Compared to ref 42, where $d = 16$ Å was used, the concentration axis for the DLS data on PBLG-277000 has been recomputed using $d = 20$ Å. These polymers are close enough in size, and large enough, that scaling the friction by L should be adequate. Mutual behavior and self-behavior clearly differ at low concentrations; f_m rises immediately with concentration, while f_s is initially level. At high concentrations, the two friction factors approach each other and perhaps f_s slightly exceeds f_m (especially since f_m is slightly overestimated because a correction term[67] of $(1-\phi)^2$ was not used). Similar analysis for lower-mass polymers confirms the difference at low concentration and suggests that f_s could become much larger than f_m. However, the appropriateness of scaling the friction by length is questionable for the smaller polymers. Mutual friction data at very high concentrations are not available for the fluorescently tagged samples, so a really correct comparison between self-friction and mutual friction of low-M rods cannot be made.

Altenberger and Tirrell[68] have reviewed the differences between f_s and f_m in terms of Kubo velocity–velocity correlation functions. For an N-solute system:

$$f_s = \frac{3kT}{\int_0^\infty dt\ \langle v_1(t)\cdot v_1(0)\rangle} \tag{18}$$

where $\langle v_1(t)\cdot v_1(0)\rangle$ is the equilibrium velocity–velocity autocorrelation function for the solute particles. By comparison

$$f_m = \frac{3kT}{\int_0^\infty dt\ [\langle v_1(t)\cdot v_1(0)\rangle + (N-1)\langle v_1(t)\cdot v_2(0)\rangle]} \tag{19}$$

The additional equilibrium solute cross-correlation term $\langle v_1(t)\cdot v_2(0)\rangle$ governs the difference between f_m and f_s. The local concentration fluctuations that mutual diffusion describes are the result of negative velocity cross-correlations, on average. To produce (dissipate) a concentrated zone, particles move together (apart). Thus, we might expect the cross-correlation term to be negative, so that $f_m > f_s$. This appears to be in agreement with available evidence for dilute to moderately concentrated solutions of poly(ethylene oxide)[69] and dextran[70] and with the present results at low concentration. As the solution becomes more concentrated, hydrodynamic screening may cause the cross-correlation term to be dominated by short-range elements, including many orthogonal velocity pairs in the semidilute, isotropic solution. The magnitude of the cross-correlation term would be reduced and f_m would approach f_s. At sufficiently high concentrations, locally oriented rods may enjoy coupled motions, leading to a positive cross-correlation term and bringing f_m to a value below f_s. In short, we propose that the cross-correlation term starts out negative and approaches zero. The evidence for a positive cross-correlation term at very high concentrations is still feeble, although the concept is reasonable for rods because of their tendency to align at high concentrations. There is an additional caveat concerning the comparisons of f_s and f_m, which is that SLS/DLS operates on a much shorter distance scale than FPR. In both experiments, attempts are made to extrapolate the results to the long distance limit, but as the solutions become very concentrated, such that pretransitional effects associated with the appearance of a liquid crystalline phase appear, this may become difficult. The problem is especially severe for SLS/DLS, since its distance scale is 2–3 orders of magnitude less than that of FPR.

The slightly nonexponential character of some FPR signals has been ignored. A number of possible explanations exist. FPR as practiced here is a "look through" technique—light from the cell edges is mixed with light fluoresced near the middle of the sample. Diffusers that bind weakly to the cell surface should spawn a separate recovery mode, with amplitude dependent on the amount of material near the edge compared to that in the middle. The presence of such diffusers can be probed by varying the cell thickness. Doubling the thickness of the cells did not significantly reduce the nonexponential character (admittedly, this evidence against surface effects depends on the noise content of the signals). Ultrasonic stimulus applied during measurement also had no effect. The polydispersity of PBLG depends sensitively on conditions during synthesis.[35,36,71] Typically, a low-M component is present that would be removed by the extensive rinsing procedures used to remove any unreacted dye. However, the main component may still not be completely monodisperse. As noted above, in concentrated solutions the molecular weight exponent for diffusion, β, approximately doubles from the empirical dilute solution value of 0.7. This would exacerbate polydispersity problems and, indeed, the nonexponentiality is worst for concentrated solutions of LPBLG-232000, the most polydisperse sample according to DLS. Even for this polymer, essentially single-exponential behavior is observed in the dilute and strongly decreasing regimes. The main conclusions of this paper are unaffected because the nonexponentiality problems begin well after the level dilute regime and strong downturn regime, beginning at $\nu/\nu^* = 0.5$. This is near the concentration where slow modes become prominent in dynamic light scattering, accompanied by a change in the concentration dependence of the correlation length from negative to positive and strong increases in the depolarized scattering. These pretransitional effects herald the imminent separation into liquid crystalline and isotropic phases.[49] At these concentrations, rotational diffusion has slowed to a near standstill as the system becomes increasingly indifferent to transient orientation near the liquid crystal boundary.[72] Under these conditions, rods will diffuse (with parallel and perpendicular com-

ponents, mostly the former) to form small, imperfectly oriented domains. Though not completely stable, these domains may last a long time and could diffuse *en masse*, causing a slow decay mode. Two-exponential fits show that the nonexponentiality actually appears to be caused by emergence of a new *fast* mode (i.e., the single-exponential fits used up to now return an ill-defined average decay rate that is close to the slower decay mode). Both fast and slow decay rates are diffusive—i.e., they scale with K^2. A possible cause for this behavior is transient fractionation. Biphasic isotropic/liquid crystalline solutions exhibit equilibrium fractionation of the larger rods into the liquid crystal phase.[73] It seems possible to form transient but fairly long-lived regions where some pretransitional fractionation may occur, thus accounting for the rapid decay mode. Experiments are being designed to understand the nonexponential recovery profiles better. At this time, the simplest explanation for the nonexponentiality of the largest LPBLG at the highest concentrations is polydispersity, made more obvious by the increasing molecular weight dependence of diffusion at high concentrations.

Conclusion

The self-diffusion of fluorescently tagged PBLG has been measured throughout the isotropic regime in pyridine, a good solvent. The self-diffusion data are not well fit by any analytical theory. Dilute behavior holds to number densities well exceeding L^{-3}, the number density usually associated with topological constraints for thin rods. The onset of topological constraints is greatly delayed, and diffusion begins to decrease at a concentration nearer to the classical overlap criterion, $[\eta]^{-1}$, particularly for the shorter rods. The criterion $\nu^+ dL^2 \approx 0.5$–1, corresponding to $\nu^+/\nu^* \approx 0.1$–0.2, is appropriate for all molecular weights studied. This implies that excluded-volume (finite thickness) effects are important at concentrations where topological constraints might become active. There was some evidence for a two-stage rolloff of diffusion for the highest molecular weights, suggesting the importance of higher axial ratios, with equal or greater stiffness, in future studies. Self-diffusion, like mutual diffusion, is reasonably well scaled when the number density is normalized by ν^*. The self-friction factor is lower than the mutual friction factor in dilute solutions. Cessation of motion at high number densities, the "intuitive picture" envisioned by Edwards and Evans and mentioned by one of us as a sort of mechanical explanation for the formation of thermoreversible gels of rods under nonequilibrium conditions,[32] was not observed for rods at equilibrium.

Acknowledgment. We thank Professor William H. Daly and Dr. Drew S. Pochè for valuable suggestions concerning the labeling of PBLG. This work has been supported by Grants DMR-8914604 and DMR-9221585 from the National Science Foundation. D.T. acknowledges the financial support of the LaSPACE program.

Supplementary Material Available: Listing of an alternate method for side-chain labeling of PBLG (illustrated in Scheme 2) and tables of D_m's of various LPBLG's in DMF measured by DLS and self-diffusion coefficients of various LPBLG's in pyridine solutions by FPR measurements (13 pages). Ordering information is given on any current masthead page.

References and Notes

(1) Graessley, W. W. *Adv. Polym. Sci.* **1982**, *47*, 67–117.
(2) Tirrell, M. *Rubber Chem. Technol.* **1984**, *57*, 522–557.
(3) Lodge, T. P.; Rotstein, N. A.; Prager, S. *Adv. Chem. Phys.* **1990**, *LXXIX*, 1–133.
(4) Phillies, G. D. J. *J. Phys. Chem.* **1989**, *93*, 5029.
(5) Lodge, T. P.; Markland, P.; Wheeler, L. M. *Macromolecules* **1989**, *22*, 3409–3418.
(6) Klein, J.; Fletcher, D. *Nature* **1983**, *304*, 526–527.
(7) Russo, P. S. In *Dynamic Light Scattering, the Method and Some Applications*; Brown, W., Ed.; Oxford: New York, 1993; pp 512–553.
(8) Tracy, M. A.; Pecora, R. *Annu. Rev. Phys. Chem.* **1992**, *43*, 525–557.
(9) Edwards, S. F.; Evans, K. E. *Trans. Faraday Soc.* **1982**, *78*, 113–121.
(10) Teraoka, I.; Hayakawa, R. J. *J. Chem. Phys.* **1988**, *89*, 6989.
(11) Semenov, A. N. *J. Chem. Soc., Faraday Trans. 2* **1986**, *82*, 317–329.
(12) Sato, T.; Teramoto, A. *Macromolecules* **1991**, *24*, 193–196.
(13) Sato, T.; Takada, Y.; Teramoto, A. *Macromolecules* **1991**, *24*, 6220–6226.
(14) Takada, Y.; Sato, T.; Teramoto, A. *Macromolecules* **1991**, *24*, 6215.
(15) Doi, M.; Edwards, S. F. *J. Chem. Soc., Faraday Trans. 2* **1978**, *74*, 560.
(16) Doi, M.; Edwards, S. F. *J. Chem. Soc., Faraday Trans. 2* **1978**, *74*, 918.
(17) Hervet, H.; Leger, L.; Rondelez, F. *Phys. Rev. Lett.* **1979**, *42*, 1681–1684.
(18) Lanni, F.; Ware, B. R. *Rev. Sci. Instrum.* **1982**, *53* (6), 905–908.
(19) Blum, F. D. *Spectroscopy* **1986**, *1* (5), 32.
(20) Scalettar, B. A.; Hearst, J. E.; Klein, M. P. *Macromolecules* **1989**, *22*, 4550.
(21) Wang, L.; Garner, M. M.; Yu, H. *Macromolecules* **1991**, *24* (9), 2368–2376.
(22) Zero, K.; Pecora, R. *Dynamic Light Scattering*; Plenum: New York, 1985.
(23) Yamakawa, H. *Modern Theory of Polymer Solutions*; Harper and Row: New York, 1971.
(24) Yamakawa, H. *Annu. Rev. Phys. Chem.* **1984**, *35*, 23.
(25) The term "enmeshment" might be more appropriate for rods.
(26) Doi, M.; Edwards, S. F. In *The Theory of Polymer Dynamics*; Anonymous, Ed.; Clarendon Press: Oxford, 1986.
(27) Bitsanis, I.; Davis, H. T.; Tirrell, M. *Macromolecules* **1990**, *23*, 1157.
(28) Mustafa, M. B.; Tipton, D. L.; Barkley, M. D.; Russo, P. S.; Blum, F. D. *Macromolecules* **1993**, *26*, 370–378.
(29) Olayo, R.; Miller, W. G. *J. Phys. Chem.* **1992**, *96*, 3152.
(30) Tinland, B.; Maret, G.; Rinaudo, M. *Macromolecules* **1990**, *23*, 596–602.
(31) de Gennes, P.-G. *Scaling Concepts in Polymer Physics*; Cornell University: Ithaca, NY, 1979.
(32) Russo, P. S.; Magestro, P.; Miller, W. G. In *Reversible Polymeric Gels and Related Systems*; Russo, P. S., Ed.; American Chemical Society: Washington, DC, 1987; pp 153–180.
(33) Ushiki, H.; Mita, I. *Polym. J.* **1981**, *13* (9), 837–844.
(34) Russo, P. S.; Cao, T. *Mol. Cryst. Liq. Cryst.* **1988**, *157*, 501–514.
(35) Mitchell, J. C.; Woodward, A. E.; Doty, P. *J. Am. Chem. Soc.* **1957**, *79*, 3955–3960.
(36) Daly, W. H.; Poche, D. S.; Negulescu, I. I. *Prog. Polym. Sci.* **1994**, *19*, 79–135.
(37) Russo, P. S.; Miller, W. G. *Macromolecules* **1984**, *17*, 1324–1331.
(38) Luzzati, V.; Cesari, M.; Spach, G.; Masson, F.; Vincent, J. M. *J. Mol. Biol.* **1961**, *3*, 566–584.
(39) Flory, P. J.; Leonard, W. J. *J. Am. Chem. Soc.* **1965**, *87*, 2102–2108.
(40) DeLoze, C.; Saludjian, P.; Kovacs, A. J.; Schermutzki, B. *Biopolymers* **1964**, *2*, 43–49.
(41) Bu, Z.; Russo, P. S. *Macromolecules* **1994**, *27*, 1187–1194.
(42) DeLong, L. M.; Russo, P. S. *Macromolecules* **1991**, *24*, 6139–6155.
(43) Jamil, T.; Russo, P. S. *J. Chem. Phys.* **1992**, *97* (4), 2777–2782.
(44) Balik, C. M.; Hopfinger, A. J. *J. Colloid Interface Sci.* **1978**, *67*, 118–126.
(45) Goebel, K. D.; Miller, W. G. *Macromolecules* **1970**, *3*, 64.
(46) Doty, P.; Bradbury, J. H.; Holtzer, A. M. *J. Am. Chem. Soc.* **1956**, *78*, 947–954.
(47) Kubo, K.; Ogino, K. *Mol. Cryst. Liq. Cryst.* **1979**, *53*, 207.
(48) Robinson, C. *Mol. Cryst.* **1966**, *1*, 467.
(49) DuPrè, D. B.; Samulski, E. T. In *Liquid Crystals, the Fourth State of Matter*; Saeva, F. D., Ed.; Marcel-Dekker: New York, 1979.
(50) Wissenburg, P.; Odijk, T.; Cirkel, P.; Mandel, M. *Macromolecules* **1994**, *27*, 306–308.
(51) Onsager, L. *Ann. N.Y. Acad. Sci.* **1949**, *51*, 627.
(52) Flory, P. J. *Proc. R. Soc. London, Ser. A* **1956**, *234*, 60.
(53) Flory, P. J. *Proc. R. Soc. London, Ser. A* **1956**, *234*, 73.
(54) Flory, P. J. *Adv. Polym. Sci.* **1984**, *59*, 2–36.

(55) Yamakawa, H. *Annu. Rev. Phys. Chem.* **1984**, *35*, 23.
(56) Schmidt, M.; Stockmayer, W. H. *Macromolecules* **1984**, *17*, 509.
(57) Kubota, K.; Tominaga, Y.; Fujime, S. *Macromolecules* **1986**, *19*, 1604.
(58) Berne, B.; Pecora, R. *Dynamic Light Scattering*; Wiley: New York, 1976.
(59) Koppel, D. E. *J. Chem. Phys.* **1972**, *57*, 4814–4820.
(60) Kubota, K.; Chu, B. *Biopolymers* **1983**, *22*, 1461.
(61) Russo, P. S.; Karasz, F. E.; Langley, K. H. *J. Chem. Phys.* **1984**, *80*, 5312–5325.
(62) Tracy, M.; Pecora, R. *Macromolecules* **1992**, *25*, 337–349.
(63) Drogemeier, J.; Hinssen, H.; Eimer, W. *Macromolecules* **1994**, *27*, 87–95.
(64) Bu, Z. Self Diffusion of Semiflexible Rodlike Poly(γ-benzyl α,L-glutamate) in Dilute and Nondilute Isotropic Solutions. Ph.D. Dissertation, Louisiana State University, Baton Rouge, LA, 1994.
(65) Keep, G. T.; Pecora, R. *Macromolecules* **1985**, *18*, 1167–1173.
(66) Doi, M.; Yamamoto, I.; Kano, F. *J. Phys. Soc. Jpn.* **1984**, *53*, 3000–3003.
(67) Vink, H. *J. Chem. Soc., Faraday Trans. 1* **1985**, *81*, 1725–1730.
(68) Altenberger, A. R.; Tirrell, M. *J. Polym. Sci., Polym. Phys. Ed.* **1984**, *22*, 909–910.
(69) Brown, W.; Stilbs, P.; Johnsen, R. M. *J. Polym. Sci., Polym. Phys. Ed.* **1983**, *21*, 1029–1039.
(70) Comper, W. D.; Preston, B. N.; Daivis, P. *J. Phys. Chem.* **1986**, *90*, 128–132.
(71) Lundberg, R. D.; Doty, P. *J. Am. Chem. Soc.* **1957**, *79*, 3961–3972.
(72) Mead, D. W.; Larson, R. G. *Macromolecules* **1990**, *23*, 2524–2533.
(73) Flory, P. J. In *Polymer Liquid Crystals*; Ciferri, A., Krigbaum, W. R., Meyer, R. B., Eds.; Academic Press: New York, 1982.